Article

Molecular Orientation and Fluorescence Studies on Naphthalene Acetate Intercalated ZnAl Layered Double Hydroxide

Wenying Shi, Min Wei, Jun Lu, Feng Li, Jing He, David G. Evans, and Xue Duan

J. Phys. Chem. C, **2008**, 112 (50), 19886-19895 • Publication Date (Web): 19 November 2008

Molecular Orientation and Fluorescence Studies on Naphthalene Acetate Intercalated Zn_2Al Layered Double Hydroxide

Wenying Shi, Min Wei,* Jun Lu, Feng Li, Jing He, David G. Evans, and Xue Duan

State Key Laboratory of Chemical Resource Engineering, Beijing University of Chemical Technology, Beijing 100029, People's Republic of China

Received: July 8, 2008; Revised Manuscript Received: October 20, 2008

This paper describes a systematic study on molecular orientation and fluorescence properties for the Zn_2Al layered double hydroxide (LDH) intercalated with α-naphthalene acetate (α-NAA) and *β*-naphthalene acetate (*β*-NAA), respectively. α-NAA and *β*-NAA intercalated Zn_2Al LDH (denoted as α-NAA LDH and *β*-NAA LDH) were prepared by the ion-exchange method and their thin films on Si substrates were obtained by the solvent evaporation method. The powder X-ray diffraction (XRD) and Fourier transform infrared spectroscopy (FT-IR) of α-NAA LDH and *β*-NAA LDH confirm the intercalation of guests between sheets of LDH. The XRD and scanning electron microscope (SEM) images of α-NAA LDH and *β*-NAA LDH thin films show that they are well *c*-oriented assembly with platelet-like morphology. UV−vis absorption and fluorescence spectra (emission, lifetime, and time resolution) indicate that the intercalated NAA is accommodated in its monomer form and depolarization factors exhibit no influence on its fluorescence emission process, which makes the evaluation for its interlayer molecular orientation reasonable and feasible by polarized fluorescence method. Fluorescence polarization method was applied to investigate the preferential orientation of the interlayer α-NAA and *β*-NAA molecules, and the results show that α-NAA and *β*-NAA are intercalated between sheets of Zn_2Al LDH as monomeric units with a tilt angle Ψ (defined as the angle between the transition moment of NAA molecule with respect to the normal to the LDH layer) of 60° and 65°, respectively. Compared with the physical mixture samples of NAA and LDH, the intercalation of NAA leads to an increase in the fluorescence lifetime. This indicates a more dilute and constrained interlayer environment for the guest, which reduces the internal mobility and the flexibility of NAA and thus improves its fluorescence lifetime.

1. Introduction

Inorganic−organic hybrid materials have attracted much attention for the last decades.[1] The possibility to combine the properties of the two components has been the driving force in materials research and application fields, in particular because they are attractive candidates for optical and electronic devices, sensor coatings, and catalysts.[2,3] For the inorganic framework, layered materials with two-dimensional arrays in the nanoscale space domain are suitable systems with interesting applications in modified electrodes, chemical sensors, photochromic devices, and nonlinear optics.[4,5] From this point of view, layered double hydroxides (LDHs) are one kind of important layered matrixes which represent a large versatility in terms of their chemical composition and layer charge.[6] LDHs can be represented by the general formula $[M^{2+}_{1-x}M^{3+}_{x}(OH)_2]^{x+}(A^{n-})_{x/n}\bullet mH_2O$, where M^{2+} and M^{3+} are metal cations and A^{n-} is an anion. The host structure consists of brucite-like layers of edge-sharing $M(OH)_6$ octahedra, and the partial substitution of M^{3+} for M^{2+} induces positively charged host layers, balanced by the interlayer anions.[7]

Recently, the immobilization of photoactive molecules and optic-functionalization of the LDHs have been reported,[8–11] and the immobilization of guest molecules with a preferential arrangement in ordered LDHs can result in a desired alignment of photofunctional molecules in a macro-scale domain. Costantino et al.[12] have reported that the fluorescence emission of the methyl orange (MO) molecule incorporated into Zn_2Al LDH covers the whole visible wavelength range by changing the dye loading, owing to the different arrangement of the interlayer MO molecule. Cooper and co-workers[13] reported the intercalation of 4-nitrohippuric acid (NHA) between sheets of LDH, and the hybrid material exhibits frequency-doubling characteristics for incident 1064 nm infrared light, due to the ordered arrangement of molecular dipole.

It was known that the arrangement of guest molecule within the host matrix is paramount, for it determines the optical, electronic, and magnetic properties of the resulting composite to a great extent.[14] Orientation investigation of interlayer guests based on experimental techniques can not only promote profound insight for host−guest interactions, but can also provide fundamental information for structural design and assembly of inorganic−organic composites with specific functionality. Routine technique, such as powder XRD, has been generally used to evaluate the arrangement of guest between sheets of LDH in previous work, which is based on the comparison between basal spacing (d_{003}) of the intercalate and the length of anion. However, this is of particularly rather low precision without taking into account the intermolecular interactions of guest, coexisting anions, moisture content, etc. Polarized fluorescence,[15–17] resulted from the ordered arrangement of chromophore guest, can be employed as a structure probe for the orientation of guest, since it provides useful information on molecular mobility, size, shape, and flexibility, fluidity of a medium, and order parameters.[18] It has been used to determine the orientation of cationic dyes incorporated in the Laponite host.[16,17] Although there have been some molecular dynamics studies on the arrangement of interlayer guest, to the best of

* Corresponding author. Phone: +86-10-64412131. Fax: +86-10-64425385. E-mail: weimin@mail.buct.edu.cn.

10.1021/jp806024n CCC: $40.75
Published on Web 11/19/2008

SCHEME 1: Molecular Structures of (A) α-NAA and (B) β-NAA

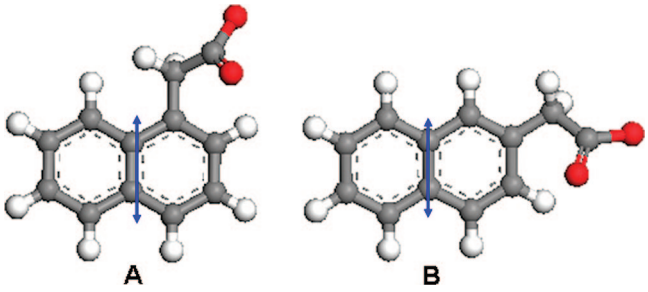

our knowledge, no experimental study with high accuracy for the orientation of guest anion in the interlayer region of LDHs has been reported.

In the present work, α-NAA and β-NAA (Scheme 1) are used as a model system for the study on the orientation of guest intercalated in LDH by the method of fluorescence polarization spectroscopy combined with XRD. It was found that the monomers of α-NAA and β-NAA are accommodated in the interlayer region as double layer and interdigitated bilayer, with a tilt angle (Ψ) of 60° and 65° respectively. Compared with the physical mixture samples of pristine α-NAA and β-NAA with LDH, the UV−vis absorption and emission fluorescence spectra of the intercalated α-NAA and β-NAA indicate that the NAA anions are located in a more dilute microenvironment. Moreover, the increase in fluorescence lifetime of the intercalated NAA roots in a more rigid and constrained environment due to the host−guest and guest−guest interactions, indicating the decreases in the internal mobility and flexibility of the guest, as well as the reduction in its internal conversion processes. On the one hand, photoresponse of NAA intercalated LDH provides information on the interlayer organization and microenvironment of the guest; on the other hand, the orientation of the interlayer guest leads to the specific photochemical properties of the composite. Therefore, this work not only provides a detailed understanding for the influences of host−guest and guest−guest interactions on the orientation of interlayer chromophore guest, but also presents potential applications of lamellar organic−inorganic composites with interesting photochemical and photophysical properties based upon organic chromophore regularly arranged within an inorganic matrix.

2. Experimental Section

2.1. Materials. Analytical grade chemicals including sodium α-NAA, sodium β-NAA, $Zn(NO_3)_2 \cdot 6H_2O$, $Al(NO_3)_3 \cdot 9H_2O$, NaOH, and so forth were purchased from the Beijing Chemical Co. Limited, and used without further purification. The deionized and de-CO_2 water was used in all these experimental processes.

2.2. Synthesis of the NAA Intercalated Zn_2Al LDH. The Zn_2Al-NO_3 LDH precursor was synthesized by the hydrothermal method reported previously.[19] The pH of aqueous solution (200 mL) containing 0.08 mol $Zn(NO_3)_2 \cdot 6H_2O$ and 0.04 mol $Al(NO_3)_2 \cdot 9H_2O$ was adjusted to 8.5 with $NH_3 \cdot H_2O$, and it was aged in an autoclave at 140 °C for 10 h. The precipitate was centrifuged and washed thoroughly with water. Subsequently, the α-NAA and β-NAA intercalated LDH were prepared following the ion-exchange method. Freshly prepared Zn_2Al-NO_3 LDH (0.5 g) was added to an aqueous solution of α-NAA (150 mL, pH = 8.0); the mixture was held at room temperature under N_2 atmosphere for 48 h. The product α-NAA LDH was washed extensively with water. The β-NAA intercalated LDH was synthesized following the same procedure.

2.3. Fabrication of α-NAA LDH and β-NAA LDH Thin Films. Thin film of α-NAA LDH was fabricated by solvent evaporation method. Substrates of Si wafer were first cleaned by immersing in a bath of H_2SO_4/H_2O_2 (3/1, v/v) and then were treated in an ultrasonic bath for 30 min. Pasty α-NAA LDH (0.05 g) was suspended in water (20 mL) in a glass flask and treated in an ultrasonic bath (99 W, 28 kHz) under N_2 atmosphere for 5 min. Then, the resulting α-NAA LDH suspension was dropped on Si substrates and dried in vacuum at ambient temperature for 5 h. The thin film of β-NAA LDH was fabricated following the same procedure.

2.4. Techniques of Characterization. The powder XRD measurements were performed on a Rigaku XRD-6000 diffractometer, using Cu Kα radiation ($\lambda = 0.15418$ nm) at 40 kV, 30 mA, with a scanning rate of 5°/min, and a 2θ angle ranging from 2° to 65°. SEM images were obtained using a Hitachi S-4700 scanning electron microscope operating at 20 kV. Metallic elemental analysis was performed by atomic emission spectroscopy with a Shimadzu ICPS-7500 instrument. C, H, and N content was determined using an Elementar vario elemental analysis instrument.

Fluorescent Decay. The curves were recorded by means of the time-correlated single-photon counting technique employing a LifeSpec-red lifetime spectrometer (Edinburgh Instruments Ltd. UK), which is equipped with an emission double monochromator and a time resolution of 25 ps after deconvolution of the excitation pulse. From the recorded fluorescent decay curves, two different analyses can be performed for the recorded data considering two experimental setups:[20]

(i) Fluorescence Lifetime Analysis. For a fixed emission wavelength, the fluorescence decay curve was collected up to 60 000 counts at the channel with the maximum emission. The lifetime of the samples was obtained from the recorded decay curves after deconvolution of the instrument response function (IRF) carried out by an iterative method of nonlinear least-squares based on the Marquardt algorithm. The decay curves were adjusted to a sum of exponential decays (i.e., as multiexponentials) by means of:

$$I_{flu}(t) = A_1 \exp\left(-\frac{t}{\tau_1}\right) + A_2 \exp\left(-\frac{t}{\tau_2}\right) + \ldots \qquad (1)$$

where A_i are the preexponential factors related with the statistical weights of each exponential and τ_i are the lifetimes of each exponential decay. The goodness of the deconvolution process was controlled by related coefficients (r^2) and the residual analysis. The fluorescence decay curves were analyzed at emission wavelength of 337 nm for α-NAA LDH and β-NAA LDH.

(ii) Time-Resolved Emission Spectra (TRES). Fluorescence decay curves were recorded as a function of the emission wavelength in the range 320∼385 nm for α-NAA LDH and 320∼498 nm for β-NAA LDH (wavelength increment of 1 nm) for a fixed recording time (200 s per wavelength). The emission spectra at different times after excitation were obtained by averaging the integrated fluorescence intensity for fixed time-windows of 1 ns at every wavelength in the 8 ns time interval (9 time-window spectra) for α-NAA LDH and β-NAA LDH after the 281 nm excitation pulse (ps).

Fluorescence Polarization. The spectra were recorded on a Quanta Master-Spectrofluorometers (model QM-4/2005), equipped with automated polarizers in both the excitation and the emission beams (see Figure S1 in Supporting Information). The fluorescent spectra of the thin film were registered after excitation at 281 nm for α-NAA LDH and β-NAA LDH, where the

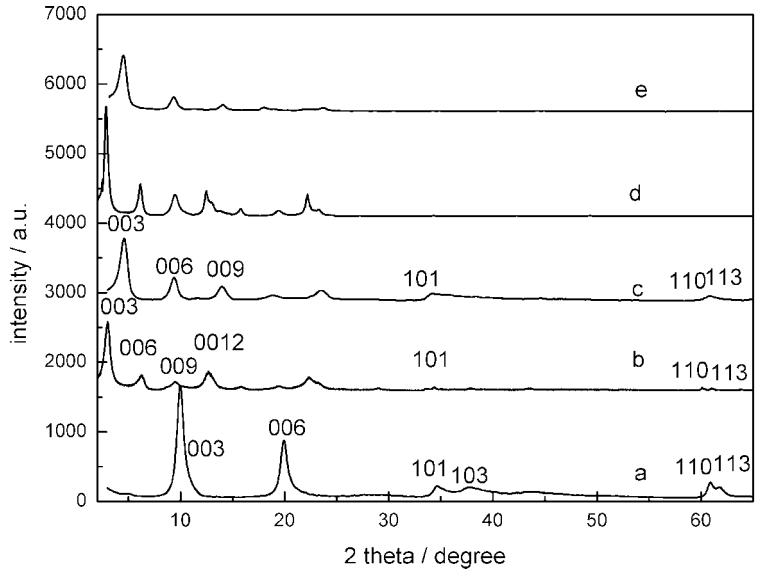

Figure 1. XRD patterns for (a) Zn_2Al-NO_3 LDH powder, (b) α-NAA LDH powder, (c) β-NAA LDH powder, (d) α-NAA LDH thin film, and (e) β-NAA LDH thin film.

fluorescence emission was collected along the z' axis at 90° with respect to the excitation beam in the z axis. The fluorescence polarization spectra were scanned in the range 320∼410 nm for α-NAA LDH and 325∼440 nm for β-NAA LDH every 1 nm, with an integration time of 2 s and excitation and emission slits of 8 nm.

The orientation of the thin film with respect to the excitation beam was changed by rotating the solid-sample holder around its vertical y axis. Indeed, the angle between the normal to the thin film and the excitation axis (defined as the δ angle) was scanned from 30 to 70° for α-NAA LDH and from 50 to 90° for β-NAA LDH. The instrumental response to the linearly polarized light has been corrected by recording the fluorescent signal of an isotropic system under identical experimental conditions. In the present work, a 2.5×10^{-5} M aqueous solution of α-NAA and a 3.0×10^{-5} M solution of β-NAA were used as isotropic system for the thin films of α-NAA LDH and β-NAA LDH, respectively.

3. Results and Discussion

3.1. Macroscopic Orientation of α-NAA LDH and β-NAA LDH. The XRD patterns of Zn_2Al-NO_3 LDH, α-NAA LDH and β-NAA LDH are shown in Figure 1. In each case, the XRD patterns exhibit the characteristic reflections of the LDH structure with a series of (00l) peaks appearing as narrow, symmetric, strong lines at low angle. The basal spacing of Zn_2Al-NO_3 LDH (Figure 1a) powder sample is 0.87 nm, which is similar to the value reported previously.[21] The basal spacing expands to 2.80 and 1.94 nm (Figure 1b,c), when NO_3^- is replaced by α-NAA and β-NAA in an ion-exchange reaction, respectively, indicating that the two compounds have been successfully intercalated into the interlayer region. This is in accordance with the results of FT-IR spectra (see Figure S2 in Supporting Information). The chemical compositions are $[Zn_{0.68}Al_{0.31}(OH)_{1.98}](NO_3)_{0.16}(\alpha\text{-NAA})_{0.15}\cdot 1.32H_2O$ for α-NAA LDH and $[Zn_{0.68}Al_{0.31}(OH)_{1.98}](NO_3)_{0.14}(\beta\text{-NAA})_{0.17}\cdot 1.08H_2O$ for β-NAA LDH, obtained from the results of elemental analysis, ICP-AES and TG-DTA. It can be seen that the XRD patterns for powder form of Zn_2Al-NO_3 LDH (Figure 1a), α-NAA LDH (Figure 1b) and β-NAA LDH (Figure 1c) show (10l) and (11l) reflections indicative of LDH host sheets. In contrast, the strong basal reflections (00l), narrow half-peak breadth and the absences of any nonbasal reflections (h, $k \neq 0$) for the thin films of both α-NAA LDH (Figure 1d) and β-NAA LDH (Figure 1e) are as expected for extremely well c-oriented assembly of LDH platelets.[22,23] It can be seen from Figure 1 that the (003) reflection of the thin film sample moves to lower 2θ value compared with its powder sample. This might be related to the different content of interlayer water between them. Although the drying temperatures for the two samples are the same during the synthesis process, the c orientation of NAA LDH platelets immobilized on the surface of substrate may inhibit the evaporation of interlayer water molecules and thus a larger interlayer distance (d_{003}) can be observed.

SEM images of the α-NAA LDH and β-NAA LDH are displayed in Figure 2. The powder samples of α-NAA LDH and β-NAA LDH afford a rough surface and high magnification SEM images (Figure 2a,b) reveal that they are composed of randomly oriented LDH particles with irregular morphology. In contrast, the thin films of α-NAA LDH and β-NAA LDH exhibit a surprisingly smooth and continuous surface in the top view (Figure 2c,e). High magnification SEM images of the thin films (Figure 2d,f) demonstrate that the individual α-NAA LDH and β-NAA LDH platelets are densely packed on the substrate plane. The SEM images confirm that the thin films are constructed with well c orientation of α-NAA LDH and β-NAA LDH platelets, consistent with the XRD results in Figure 1.

3.2. Photoproperties of NAA before and after Intercalation into LDH. ***3.2.1. Orientation of Transition Dipole Moments for NAA.*** In most cases, the transition moment can be denoted as a vector in the coordinate system defined by the location of atomic nuclei; therefore, the molecules whose absorption transition moments are parallel to the electric vector of a linearly polarized incident light are preferentially excited. The probability of excitation is proportional to the square of the scalar product of the transition moment and the electric vector. This probability thus reaches its maximum when the two vectors are parallel or becomes zero when they are perpendicular.

For π-π^* transitions of aromatic hydrocarbons, the absorption transition moments are in the plane of the molecule, whose direction with respect to the molecular axis depends on the

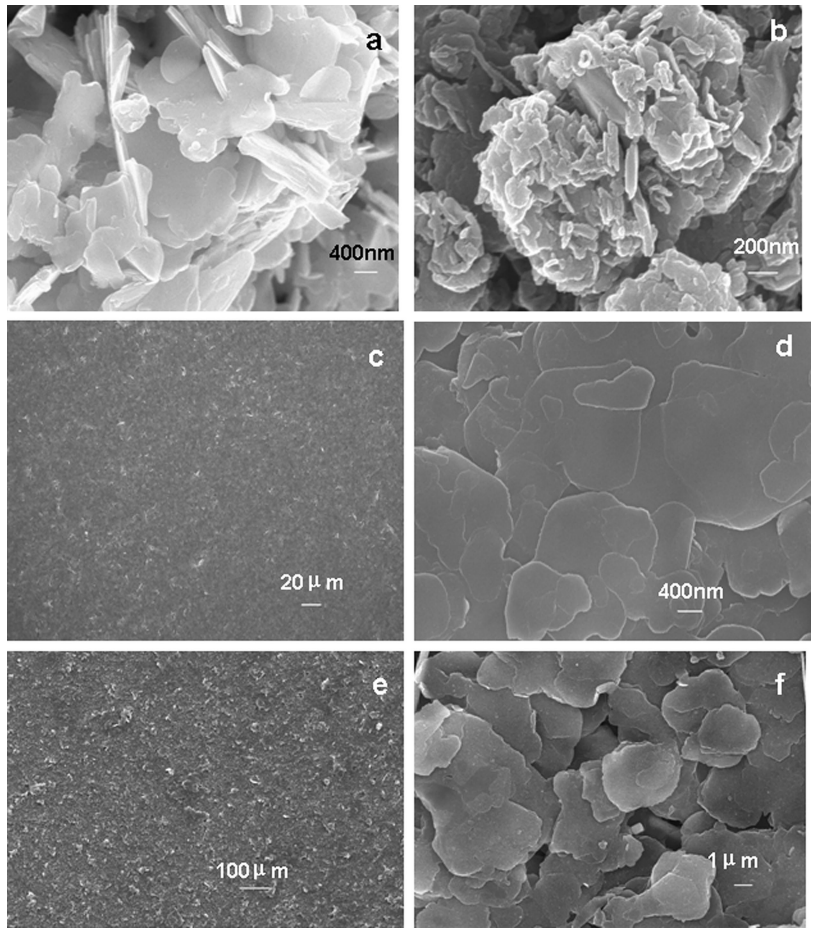

Figure 2. SEM images for (a) α-NAA LDH powder; (b) β-NAA LDH powder; α-NAA LDH thin film at (c) low and (d) high magnification; β-NAA LDH thin film at (e) low and (f) high magnification.

electronic state attained on excitation. In the case of naphthalene and anthracene, the transition moment is oriented along the short axis for the $S_0 \rightarrow S_1$ transition and along the long axis for the $S_0 \rightarrow S_2$ transition.[24] Indeed, the main absorption band and the fluorescence emission of NAA involve $S_0 \rightarrow S_1$ singlet states.[25] Therefore, both transitions are oriented along the short molecular axis, as quantum mechanic calculations suggested, and this is illustrated in the molecular structure of NAA (as shown in Scheme 1).

3.2.2. Optical Absorption and Fluorescence Spectra of NAA in Solution and Solid State. The UV−vis absorption spectra of NAA in solution and solid state samples (physical mixture of NAA and LDH, and NAA intercalated LDH respectively) were measured and displayed in Figure 3. The UV−vis absorption band of solid samples (curve b and c in Figure 3A and Figure 3B) is broader than that of NAA solution sample (curve a in Figure 3A and Figure 3B). The width of absorption band for the intercalated NAA is the result of homogeneous broadening due to the existence of a continuous set of vibrational sublevels in each electronic state.[26] The absorption spectrum of the physical mixture of α-NAA and LDH (curve b in Figure 3A) shifts to longer wavelength (ca. 14 nm) with respect to the solution sample (curve a in Figure 3A). In the case of the mixture of β-NAA and LDH (curve b in Figure 3B), the similar phenomena was found with a red-shift of 9 nm. The shift is contributed to the order and dense packing of NAA molecules, which results from NAA intermolecular interactions, especially $\pi-\pi$ interaction.[14] In contrast, the spectra of the intercalated NAA in LDH (curve c in Figure 3A and Figure 3B) do not show any shift caused by intermolecular interactions presenting in the mixture samples, demonstrating that NAA molecules are accommodated between the sheets of the host matrix mainly as monomer form. Therefore, the depolarization of fluorescence will be avoided because of transfer of the excitation energy to adjacent molecules.

The monomer form of NAA molecule in the interlayer region can also be confirmed from the fluorescence spectra. Compared with monomer of either α-NAA or β-NAA in solution, no significant change in the position of the fluorescence maximum (337 nm) was observed when they were intercalated into LDH respectively. However, the full width at half-maximum (fwhm) of fluorescence peak for the intercalated samples is larger than that of solution samples (data not shown). This is a general observation for dyes in solid-state samples and is ascribed to changes in the vibronic states of the electronic states in rigid media.[27] Moreover, an orientation distribution between the naphthalene rings with respect to the main plane of the NAA molecule, as a consequence of the restricted interlayer space in LDH, could contribute to the broadening of the fluorescence peak. In this case, a distribution of energy levels for the excited-state of the monomer NAA can exist.[28–32] This argument is consistent with the fluorescence decay curves (see 3.2.3 section), since they cannot be analyzed as uniexponential decay curves for both α-NAA LDH and β-NAA LDH.

3.2.3. Fluorescence Lifetime of the Intercalated NAA. To gain an in-depth insight into the solid state photophysical properties, fluorescence lifetime for NAA intercalated LDH was studied (Figure 4), and typical fitting results of the fluorescence

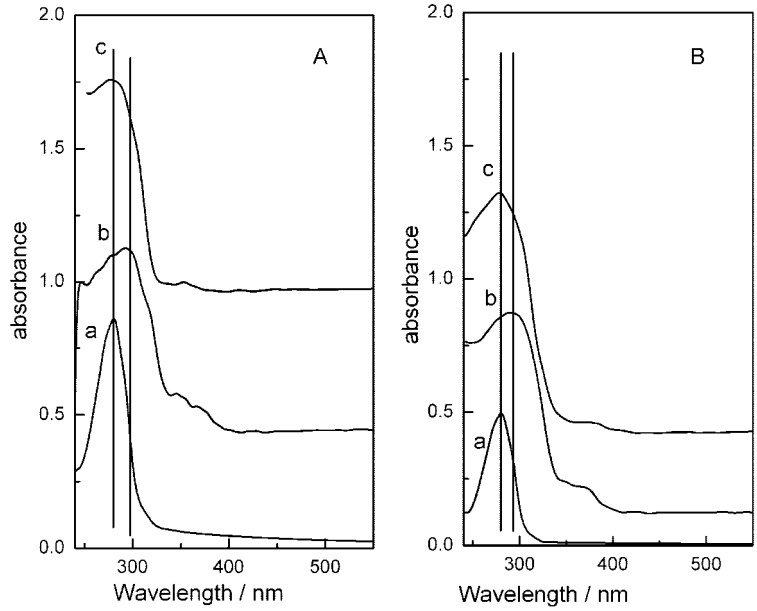

Figure 3. (A) UV−vis absorption spectra of α-NAA for (a) in solution, (b) mixed with LDH, and (c) intercalated in LDH; (B) β-NAA for (a) in solution, (b) mixed with LDH, and (c) intercalated in LDH.

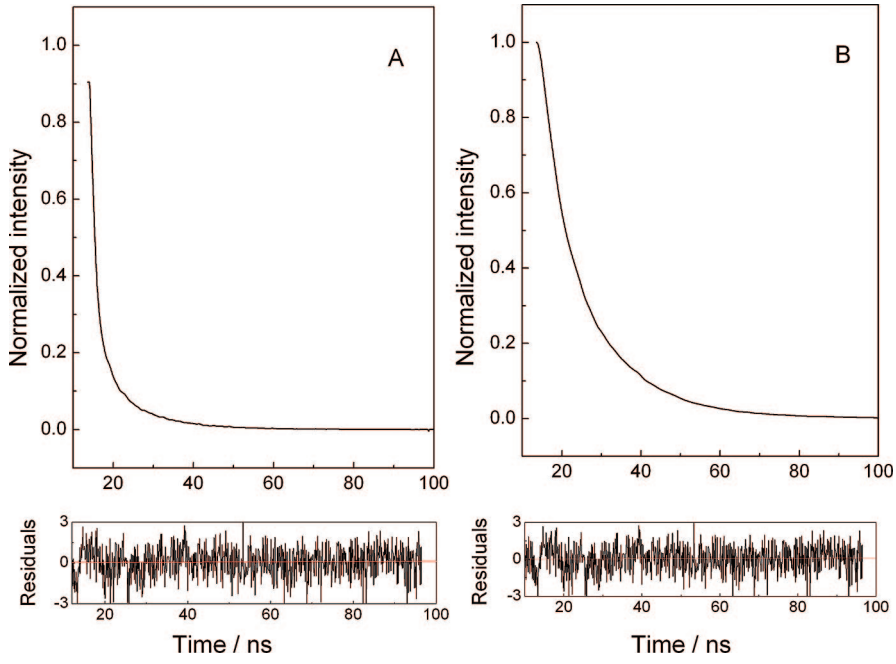

Figure 4. Fluorescence decay curves and residual plots of fits with biexponential for (A) the intercalated α-NAA and (B) the intercalated β-NAA.

TABLE 1: Fitting Fluorescent Lifetime Parameters for the Intercalated α-NAA and β-NAA

	intercalated α-NAA	intercalated β-NAA
Chi^2/Dof	0.00003	0.00002
r^2	0.9993	0.9995
A_1	4.05/77%	7.23/79%
A_2	1.15/23%	1.93/21%
τ_1/ ns	6.91	6.60
τ_2/ ns	16.2	15.5
$<\tau>$/ ns	9.04	8.51

decay curves at 337 nm are listed in Table 1. It can be seen that both the fluorescence decay curves are well-fitted by biexponential function with $r^2 > 0.99$ and the weighted residuals were randomly distributed about zero. This multiexponential behavior cannot be ascribed to a reorientation of the monomer and surrounding molecules during the initial period after excitation, because the fluorescence curves recorded with horizontal and vertical polarization (not shown) remain identical. This suggests that, in the excited state, both the intercalated α-NAA and the β-NAA molecules do not reorient or preferentially orient with respect to the polarized excitation light. The multiexponential decay curves are usually observed in solid samples, and they can be attributed to the highly heterogeneous environments for the molecules in the solid surfaces.[33,34] Indeed, several host−guest interactions occur between NAA molecule and LDH: electrostatic interaction, hydrogen bonding formed among NAA, hydroxyl groups of LDH and interlayer water. Similar conclusion has been reported by other researchers in

the study of intercalation of Rhodamine 6G (R6G) into Laponite clay.[20] Because of the difficulty in giving an appropriate interpretation for multiexponential decay curves, an average lifetime was estimated by means of[35]

$$\langle \tau \rangle = \frac{\sum_{i=1}^{n} A_i \tau_i^2}{\sum_{i=1}^{n} A_i \tau_i} = \sum_{i=1}^{n} f_i \tau_i \quad (2)$$

$$\sum_{i=1}^{n} f_i = 1 \quad (3)$$

where A_i has been defined in eq 1. The intensity average lifetime represents the average time in which the molecules are in the excited state.[36]

The average lifetimes of the α-NAA LDH and β-NAA LDH samples at the emission maximum are 9.04 and 8.51 ns (Table 1), respectively. Compared with the physical mixture samples (6.97 and 3.17 ns, respectively; see Supporting Information Figure S3 and Table S1), the intercalation of NAA into LDH leads to a remarkable increase in the fluorescence lifetime. This is in accordance with the result observed by absorption spectroscopy. The spectral shift in the α-NAA LDH and β-NAA LDH systems coupled with longer luminescence lifetime indicates a more dilute guest microenvironment. Meanwhile, a more rigid and constrained environment due to the hydrogen bonding and electrostatic interaction between NAA and LDH layers reduces the internal mobility and flexibility of naphthalene acetate molecule, decreasing the internal conversion process and thus improving its fluorescence lifetime.

3.2.4. Time-Resolved Emission Spectra of NAA LDH. Time-resolved emission spectroscopy is also a valid method to get the information on the structure of the NAA molecule intercalated into LDH. Figure 5A,B (α-NAA LDH, β-NAA LDH) shows that the peak at 337 nm does not change with increasing delay time from 0 to 8 ns. The result rules out the presence of different α-NAA and β-NAA species with different emission energies. Note that time-resolved measurements confirm the results obtained by UV−vis absorption and steady-state fluorescence spectral measurement that the NAA molecule is intercalated into the inorganic matrix mainly as the monomer form. In addition, the absence of time-dependent fluorescence anisotropy reveals that both the α-NAA and the β-NAA molecules do not reorient or readsorption in the time scale of the fluorescence lifetime.

3.3. Orientation of NAA Intercalated in LDH. It is known that the XRD technique can only provide a rough estimation of the orientation angle for the intercalated molecule in LDH, for molecular interactions are not considered (e.g., aggregation phenomena), which may result in different anion species (such as dimers, trimers, and/or oligmer aggregates) with different geometries and species sizes. In this work, the preferential orientations of α-NAA and β-NAA intercalated LDH were studied respectively by fluorescence polarization method. The horizontal (H) and vertical (V) polarized fluorescence spectra were recorded for a common horizontally polarized excitation light as a function of the twist angle δ of the thin film with respect to the excitation (and emission) beam. A linear relationship between the fluorescence dichroic ratio (D_{HV} defined as the ratio of H and V polarized emission spectra, $D_{HV} \equiv I_{HH}/I_{HV}$) and the twist angle δ (a right-angle configuration between the excitation and the emission beam) was established by means of[16,17]

$$D_{HV} = \frac{I_{HH}}{I_{HV}} = 2\cot^2 \psi + (1 - 2\cot^2 \psi)\cos^2(90 + \delta) \quad (4)$$

From the corresponding slope and/or intercept, the relative orientation of the intercalated NAA molecule can be evaluated by the Ψ angle (defined as the angle between the transition moment of NAA molecule and the normal to the LDH layer).

However, eq 4 is no longer valid if some depolarization phenomena occur during the fluorescent emission process. The most important depolarization processes effecting eq 4 are (a) nonparallel orientation between the absorption and the fluorescence transition dipole moments of the fluorophore; (b) excitation energy migration and/or transfer processes or any reemission phenomena, which could induce a change in the orientation of the transition moment from the excited-state directly populated in the excitation process to the fluorescence excited state

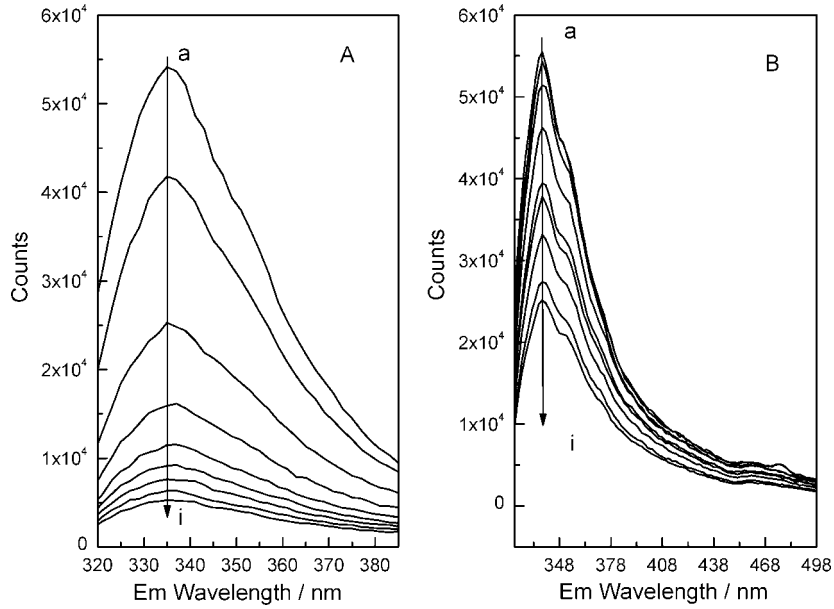

Figure 5. Time-resolved emission spectra for the sample of (A) α-NAA LDH and (B) β-NAA LDH; spectra were record from 0 (curve a) to 8 ns (curve i) after excitation at every 1 ns intervals (9 time-window spectra, respectively).

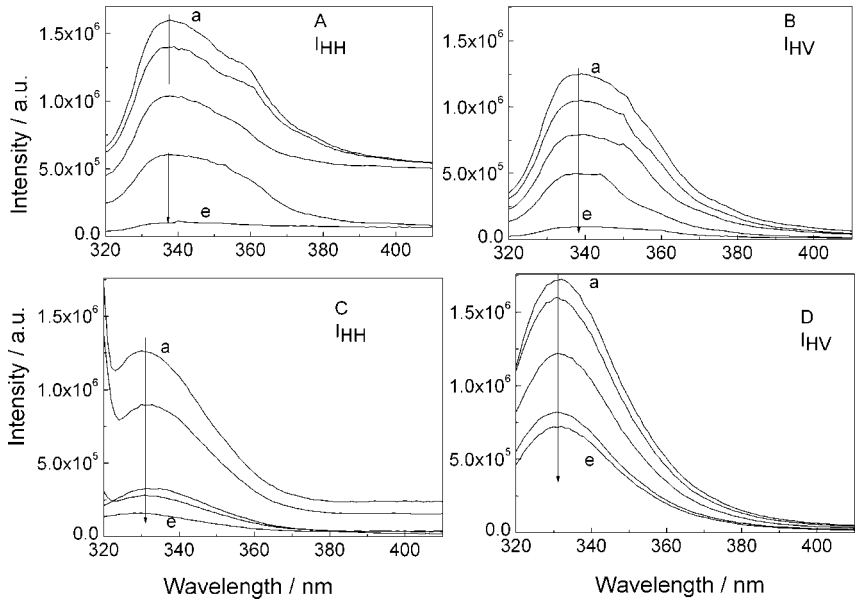

Figure 6. Evolution of the H (A) and V (B) polarized fluorescence spectra of the α-NAA LDH thin film with the following twist angles δ of the sample: (a) 30, (b) 40, (c) 50, (d) 60, and (e) 70°; evolution of the H (C) and V (D) polarized fluorescence spectra of the β-NAA LDH thin film with the following twist angles δ of the sample: (a) 50, (b) 60, (c) 70, (d) 80, and (e) 90°. Spectra were recorded after excitation with horizontal polarized light.

of the recorded emission intensity; and (c) other trivial cause of depolarization such as light scattering, reabsorption, and reemission phenomena.

In our experiment, none of the a and b phenomena are present for α-NAA LDH and β-NAA LDH with 48.3% and 54.8% anion-exchange capacity, respectively (see 3.1 section). For the c phenomenon, the influence of the light scattering could be more important at emission peaks close to the excitation energy. This effect should be more crucial for the emission polarizer with the same orientation to that used in the excitation beam (e.g., V-emission vs V-excitation in the present case) than for the crossed configuration for excitation and emission polarizer (H-emission vs V-excitation). This effect can, to some extent, be reduced by the isotropic G factor used to correct the instrumental response to the polarized light.

Figure 6 displays the fluorescence spectra of α-NAA LDH and β-NAA LDH thin films recorded with the emission polarizer in the H (I_{HH}) and V (I_{HV}) directions for different twist δ angles. These fluorescence spectra were corrected for the instrumental response to the emission H and V polarizer, taking into account the evolution of the fluorescence band of an isotropic system with the twist angle δ recorded under identical conditions. The fluorescence intensity for the emission H polarizer decreases by increasing the twist angle δ from 30° up to 70° for α-NAA LDH (Figure 6A) and from 50° up to 90° for β-NAA LDH (Figure 6C). These evolutions are also observed for the V polarized emission light (Figure 6B,D). These evolutions corroborate the fluorescence anisotropy behavior of α-NAA LDH and β-NAA LDH thin films, which are assigned to the preferential orientation of the interlayer NAA molecules.

The fluorescence anisotropy is analyzed by the dichroic parameter (D_{HV}). Because of the intrinsic instrumental response to the plane of the polarized light, D_{HV} has to be corrected for the response of the detection channel to the H and V polarization, by means of $(D_{HV})^{cor} = I_{HH}/I_{HV} \times G$ (G is the instrumental G factor determined by the recorded fluorescence anisotropy of an isotropic system, $G \equiv (I_{HV}/I_{HH})^{iso}$). In this work, solutions of pristine α-NAA and β-NAA were used as the isotropy system respectively (see Experimental Section for further details). The evolution of the fluorescence dichroic ratio with the emission wavelength of α-NAA LDH and β-NAA LDH thin films for different twist angles δ is shown in Figure 7A,B, respectively. For a given δ angle, the $(D_{HV})^{cor}$ value is practically independent of the emission wavelength, confirming the presence of only one type of α-NAA and β-NAA species for these experimental samples. The augmentation of the $(D_{HV})^{cor}$ value at shorter wavelengths for small δ angles can be attributed to an incomplete correction of the scattering of the excitation light observed in thin film samples (not shown). Actually, at those emission wavelengths close to the excitation wavelength (281 nm), this can not be corrected for the isotropic factor, because the light scattering of a solution sample in a quartz cell is much lower than that of the solid thin film.

For a given emission wavelength, the dichroic ratio of either α-NAA LDH or β-NAA LDH thin film sample linearly correlates with the $\cos^2(90 + \delta)$ value, as shown in the inset of Figure 7A at 370 nm and Figure 7B at 351 nm. According to the previously developed eq 4, the orientation Ψ angle between the transition moment of the fluorescent species and the normal to the LDH layer can be evaluated from the slope and/or intercept of this linear relationship:

$$(DHV)^{cor} = \frac{I_{HH}}{I_{HV}} \times G = 2\cot^2\psi + (1 - 2\cot^2\psi)\cos^2(90 + \delta) \quad (5)$$

The good linear relationship observed in this representation, with a correlation coefficient $r = 0.9913$ for α-NAA LDH and $r = 0.9746$ for β-NAA LDH, indicates the validity of the above assumptions related with the absence of any depolarization phenomena during the excited-state lifetime of the two thin film samples as well as the successful application of the fluorescence polarization method to evaluate the orientation of α-NAA and β-NAA molecules intercalated in LDH. Similar plots were observed for other emission wavelengths. From the slope and intercept of the $(D_{HV})^{cor}$ versus $\cos^2(90 + \delta)$ linear relationship shown in the inset of Figure 7A,B, the orientation Ψ angle of the transition moment of NAA monomer with respect to the normal to the LDH layer was calculated to be 60° for α-NAA

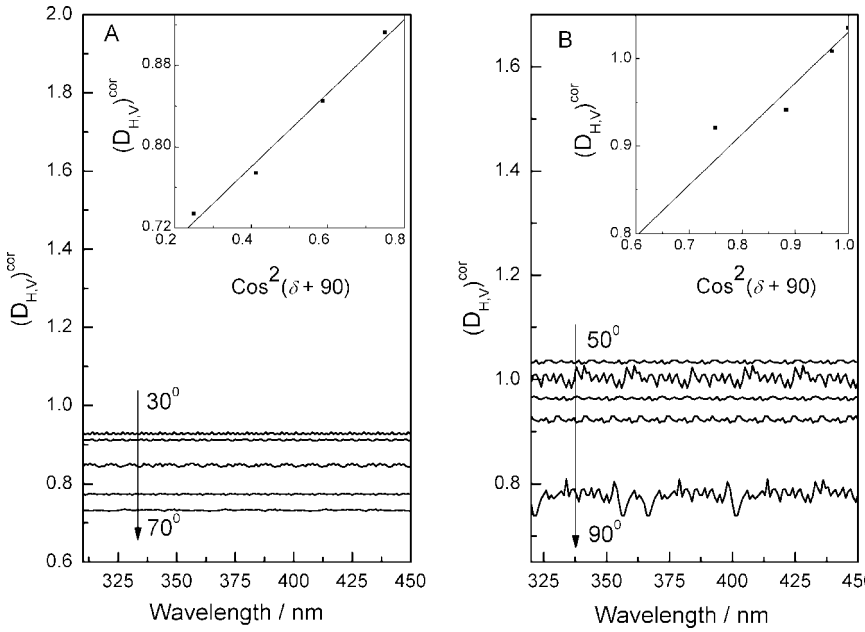

Figure 7. Evolution of the fluorescence dichroic ratio of the α-NAA LDH (A) and *β*-NAA LDH (B) thin films with the emission wavelength for different twisting *δ* angles of the sample (see Figure 6 caption). The linear relationship between the dichroic ration and $\cos^2(\delta + 90)$ at 370 nm for α-NAA LDH and at 351 nm for *β*-NAA LDH is included in the inset graph.

TABLE 2: Structural Parameters for α-NAA LDH and *β*-NAA LDH

	basal spacing/nm	lattice parameter		molecular length/nm	*ψ*/°	average distance of adjacent Al^{3+}/nm	average distance of adjacent naphthalene ring/nm
		a/ nm	*c*/ nm				
α-NAA LDH	2.80	0.31	8.39	1.01	60	0.93	0.80
β-NAA LDH	1.94	0.30	5.28	1.07	65	0.90	0.82

and 65° for *β*-NAA, respectively. The existence of acetate group in this work not only functionalizes the naphthalene molecule for intercalation but also imposes influences on the electronic structure, intramolecular charge transfer, and orientation of the dipole moment of NAA. As a result, the position of acetate group affects the preferential orientation of NAA molecule in the interlayer region of LDH.

3.4. Molecular Models of α-NAA and *β*-NAA Intercalated LDH. Based on the experimental conditions with a solution pH of 8.0, NAA molecule exists mainly as monovalent anion ($pK_a = 4\sim5$) during the ion-exchange process. The d_{003} spacing of α-NAA LDH and *β*-NAA LDH is 2.80 and 1.94 nm (Table 2), respectively. If the thickness of the LDH layer (0.21 nm[37]) and the hydrogen bonding space between the layers and the anions (0.27 nm[37]) is subtracted from the basal spacing, the values of gallery height are calculated to be 2.32 nm for α-NAA LDH and 1.46 nm for *β*-NAA LDH, which are larger than the length of the α-NAA and *β*-NAA anion, respectively (1.01 nm for α-NAA and 1.07 nm for *β*-NAA, calculated by Chemwin 6.0). Comparison of the length of the α-NAA and *β*-NAA anion with the gallery height suggests that α-NAA and *β*-NAA are accommodated in the interlayer region as double layer and interdigitated bilayer, respectively, in which the carboxyl group of individual anion interacts electrostatically with Al^{3+} cation in the LDH layers. FT-IR spectroscopy confirms the formation of hydrogen bonding system in the NAA intercalated LDH materials. The FT-IR spectra of Zn_2Al-NO_3 LDH, pristine α-NAA, α-NAA LDH, pristine *β*-NAA, and *β*-NAA LDH are shown in Figure S2. Compared with the pristine α-NAA (Figure S2b), the symmetric and asymmetric carboxylate stretching bands of the intercalated α-NAA (Figure S2c) shift to lower frequency (1407 to 1376 cm^{-1}, 1693 to 1542 cm^{-1}), indicating that the carboxylate group in α-NAA is involved in the hydrogen bonding. Moreover, compared with the Zn_2Al-NO_3 LDH precursor, the O−H stretching absorption band of α-NAA LDH shifts to lower frequency, that is, from 3519 cm^{-1} of the former (Figure S2a) to 3417 cm^{-1} of the latter (Figure S2c). This indicates that the hydroxyl group of LDH host layers participates in the formation of hydrogen bonding. In the case of *β*-NAA LDH, similar shifts can be observed. The results above indicate the formation of hydrogen bonding system among the −OH group of LDH host and $-COO^-$ of NAA anions as well as interlayer water molecules. The orientation Ψ angle of the transition moment of NAA monomer with respect to the normal to the LDH layer was calculated to be 60° for α-NAA and 65° for *β*-NAA, respectively, based on the fluorescence polarization method. On the basis of the discussion above, the suggested illustrations for the orientations of the α-NAA LDH and *β*-NAA LDH (Zn:Al = 2:1) are shown in Figure 8A,B, respectively.

3.5. Effects of Molecular Orientation on Photochemical Properties of NAA LDH. The structural parameters for the intercalates are listed in Table 2. It is known that the average distance of d_{Al-Al} is equal to 3*a* (*a* is the lattice constant of LDH) for the octahedral layer of LDH with $Zn^{2+}/Al^{3+} = 2$. Furthermore, Sideris et al. have studied the cation ordering in LDHs by multinuclear NMR spectroscopy and reported that the Mg and Al cations are not randomly distributed and there are no $Al^{3+}-Al^{3+}$ contacts in the hydroxide layers in the LDH sheets with Mg:Al = 2:1.[38] Therefore, a cation ordered host layer was chosen in this work. For α-NAA LDH with the hexagonal unit cell $a = 0.31$ nm, the average distance of d_{Al-Al} is 0.93 nm, and even if two α-NAA anions are located to adjacent Al^{3+} cations, the distance between them is 0.80 nm, which eliminates the $\pi-\pi$ interactions. By taking into account

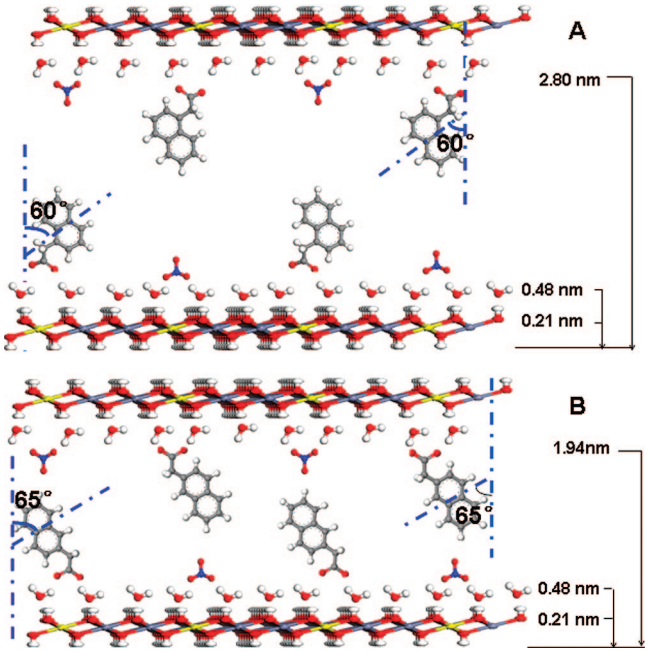

Figure 8. The suggested illustrations for the orientations of (A) α-NAA LDH and (B) β-NAA LDH. (Zn black, C grey, H white, Al yellow, O red, N blue).

the gallery height of α-NAA LDH (2.32 nm) and the length of α-NAA anion (1.01 nm), α-NAA is accommodated in the interlayer region as double layer. At the same time, the experimental XRD patterns of these samples contain rational series of basal reflections with C_0 (determines a minimum repeat distance along the c axis) ~2.32 nm characteristic for pure α-NAA-bearing LDH,[39] while the chemical analysis indicates the presence of approximately equal content of α-NAA and NO_3^- anions (see 3.1 section). From the point view of system energy, α-NAA and NO_3^- anions are possibly accommodated alternately between sheets of LDH.

The exciton theory based on monomer dipole−dipole interaction in aggregates predicts a splitting of the excited state, changing the spectroscopic characteristics of the dimmers.[40] However, red-shift in UV−vis absorption spectrum (curve c in Figure 3A) and fluorescence spectrum is not as pronounced as compared with α-NAA in solution (curve a in Figure 3A and the emission spectrum). As a result, it can be concluded that the self-aggregation of α-NAA monomers does not occur and $\pi-\pi$ interactions do not exist between adjacent α-NAA anions. Water molecules participate in the formation of hydrogen bonding system (see 3.4 section), resulting in the more dilute interlayer microenvironment than that of the physical mixture of α-NAA and LDH. Moreover, a more rigid and constrained environment reduces the internal mobility and the flexibility of NAA molecule, decreasing the internal conversion processes due to host−guest interactions, and thus improving its fluorescence lifetime and laser efficiency compared with the physical mixture sample (see 3.2.3 section).

In the case of the β-NAA LDH with $a = 0.30$ nm, if two β-NAA anions are located to adjacent Al^{3+} cations, the distance between them is 0.82 nm. The gallery height is 1.46 nm and the longest dimension of β-NAA is 1.07 nm, as a result β-NAA is accommodated in the interlayer region as interdigitated bilayer. It can be expected that the $\pi-\pi$ interactions between adjacent β-NAA anions attaching to upper and lower layers may occur, which would lead to self-aggregation of β-NAA and the spectral shift relative to the monomer's. However, this shift was not observed from the curve c in Figure 3B and the emission spectrum, indicating that $\pi-\pi$ interactions between adjacent β-NAA anions are not present. Therefore, it is reasonable to assume that the β-NAA and NO_3^- anions regularly alternate in the same layer with molar ratio of 5:4, which has been obtained from the elemental analysis (see 3.1 section). Similar to the sample of α-NAA LDH, fluorescence lifetime of β-NAA LDH increases significantly compared with that of the physical mixture sample.

4. Conclusions

The α-NAA and β-NAA molecules have been incorporated into the interlayer space of Zn_2Al-NO_3 LDH by anion exchange method, respectively, and the thin films of α-NAA LDH and β-NAA LDH were obtained by evaporating an aqueous suspension on Si substrates. The results of XRD and SEM indicate that these thin films are well c-orientated. UV−vis absorption and fluorescence spectra (emission, lifetime, and time resolution) confirm that the intercalated NAA molecule exists in monomer form without obvious $\pi-\pi$ interactions and the depolarization factors are absent during its fluorescence emission process. Therefore, the fluorescence polarization method can be successfully employed to evaluate the preferential orientation of the interlayer α-NAA and β-NAA molecules. Combined with the results of XRD, the schematic representations of the arrangement for the α-NAA LDH and β-NAA LDH are given, indicating that the monomers of α-NAA and β-NAA are accommodated in the interlayer region as double layer and interdigitated bilayer, with the Ψ angle of 60° and 65° with respect to the normal to the LDH layer, respectively.

Compared with the physical mixture samples of pristine α-NAA and β-NAA with LDH, the UV−vis absorption and fluorescence emission spectra of the intercalated α-NAA and β-NAA indicate a more dilute guest microenvironment. Furthermore, the increase in fluorescence lifetime results from a more rigid and constrained environment due to the interactions between NAA molecule and LDH layers. Therefore, this work provides a profound understanding for the influences of host−guest and guest−guest interactions on the orientation of interlayer chromophore guest. It can be expected that it offers an approach for the prospective applications of lamellar organic−inorganic composites with interesting photochemical, photophysical, and optoelectronic properties, based upon ultimately thin layers of organic chromophore regularly arranged within an inorganic matrix.

Acknowledgment. This project was supported by the National Natural Science Foundation of China, the Program for New Century Excellent Talents in University (Grant NCET-05-121), the 111 Project (Grant B07004) and the 973 Program (Grant 2009CB939802).

Supporting Information Available: Three-dimensional perspective for the experimental setup to record fluorescence spectra with linear polarized light in the front-face configuration of a PTI fluorescence instrument (Figure S1); FT-IR spectra (4000−400 cm^{-1}region) for Zn_2Al-NO_3 LDH, pristine α-NAA, α-NAA LDH, pristine β-NAA and β-NAA LDH (Figure S2); Fluorescence decay curves and residual plots of fits with biexponential for the physical mixture samples of NAA and LDH (Figure S3); Fitting fluorescent lifetime parameters for the physical mixture samples of NAA and LDH (Table S1). This information is available free of charge via the Internet at http://pubs.acs.org.

References and Notes

(1) Chem. Mater. 2001, 13 (10; Special Issue on Organic-inorganic nanocomposite materials).

(2) Gomez-Romero, P.; Sanchez, C. *Functional Hybrid Materials;* Wiley-Interscience: New York, 2003.

(3) Kickelbick, G. *Hybrid Materials, Synthesis, Characterization and Applications;* Wiley-Interscience: New York, 2007.

(4) Umemura, Y.; Yamagishi, A.; Schoonheydt, R. A.; Persons, A.; De Schryver, F. *J. Am. Chem. Soc.* **2002**, *124*, 992.

(5) Lee, H. C.; Lee, T. W.; Lim, Y. T.; Park, O. O. *Appl. Clay Sci.* **2002**, *21*, 287.

(6) Leroux, F.; Taviot-Guého, C. *J. Mater. Chem.* **2005**, *15*, 3628.

(7) Pesie, L.; Salipurovie, S.; Markovie, V.; Vucelie, D.; Kagunya, W.; Johnes, W. *J. Mater. Chem.* **1992**, *2*, 1069.

(8) Johann, B.; Peter, B.; Markus, S.; Heinz, L. *Adv. Funct. Mater.* **2003**, *13*, 241.

(9) Ukrainczyk, L.; Chibwe, M.; Pinnavaia, T. J.; Boyd, S. A. *J. Phys. Chem.* **1994**, *98*, 2668.

(10) Saito, T.; Kadokawa, J. I.; Tagaya, H. *Trans. Mater. Res. Soc. Jpn.* **2001**, *26*, 503.

(11) Hwang, S. H.; Han, Y. S.; Choy, J. H. *Bull. Korean Chem. Soc.* **2001**, *22*, 1019.

(12) Costantino, U.; Coletti, N.; Nocchetti, M.; Aloisi, G. G.; Elisei, F. *Langmuir* **1999**, *15*, 4454.

(13) Cooper, S.; Dutta, P. K. *J. Phys. Chem.* **1990**, *94*, 114.

(14) Costantino, U.; Coletti, N.; Nocchetti, M. *Langmuir* **2000**, *16*, 10351.

(15) Slyadneva, O. N.; Slyadnev, M. N.; Tsukanova, V. M.; Inoue, T.; Harata, A.; Ogawa, T. *Langmuir* **1999**, *15*, 8651.

(16) López, A. F.; Martínez, M. V. *J. Photochem. Photobiol. A. Chem* **2006**, *181*, 44.

(17) López, A. F.; Martínez, M. V. *Chem. Mater.* **2006**, *18*, 1407.

(18) Valeur, B. *Molecular Fluorescence: Principles and Applications;* Wiley-VCH: Weinheim, Germany, 2002; p 37.

(19) Bontchev, P. P.; Liu, S.; Krumhansl, J. L.; Voigt, J. *Chem. Mater.* **2003**, *15*, 3669.

(20) Martínez, M. V.; Arbeloa, F. L.; Prieto, J. B.; Arbeloa, I. L. *J. Phys. Chem. B* **2005**, *109*, 7443.

(21) Caravaggio, G. A.; Detellier, C.; Wronski, Z. *J. Mater. Chem.* **2001**, *11*, 912.

(22) Gardner, E.; Huntoon, K.; Pinnavaia, T. *Adv. Mater.* **2001**, *13*, 1263.

(23) Gursky, J. A.; Blough, S. D.; Luna, C.; Gomez, C.; Luevano, A. N.; Gardner, E. A. *J. Am. Chem. Soc.* **2006**, *128*, 8376.

(24) Valeur, B. *Molecular Fluorescence: Principles and Applications*; Wiley-VCH: Weinheim, Germany, 2002; p 27.

(25) Valeur, B. *Molecular Fluorescence: Principles and Applications*; Wiley-VCH: Weinheim, Germany, 2002; p 37.

(26) Nemkovich, N. A.; Rubinov, A. N.; Tomin, I. T., *Inhomogeneous Broadening of Electronic Spectra of Dye Molecules in Solutions*; Lakowicz J. R., Ed., Topics in Fluorescence Spectroscopy; New York, 1991; Vol. 2, 367.

(27) Valeur, B. *Molecular Fluorescence: Principles and Applications*; Wiley-VCH: Weinheim, Germany, 2002; p 67.

(28) Vuorimaa, E.; Ikonen, M.; Lemmetyinen, H. *Chem. Phys.* **1994**, *188*, 289.

(29) Vuorimaa, E.; Belovolova, L. V.; Lemmetyinen, H. *J. Lumin.* **1997**, *71*, 57.

(30) Tsukavona, V.; Lavoie, H.; Harata, A.; Ogawa, T.; Salesse, C. *J. Phys. Chem. B* **2002**, *106*, 4203.

(31) Ray, K.; Nakahara, H. *J. Phys. Chem. B* **2002**, *106*, 92.

(32) Rohatgi-Mukherjee, K. K. *Indian J. Chem.* **1992**, *31A*, 500.

(33) Rurack, K.; Hoffman, K.; Al-Soufi, W.; Resch-Genger, U. *J. Phys. Chem. B* **2002**, *106*, 9744.

(34) Wiederrecht, G. P.; Sandi, G.; Carrado, K. A.; Seifert, S. *Chem. Mater.* **2001**, *13*, 4233.

(35) Lakowicz, J. R. *Principles of Fluorescence Spectroscopy, 2d ed.;* Kluwer Academic: New York, 1999.

(36) Valeur, B. *Molecular Fluorescence. Principles and Applications;* Wiley-VCH: Weinheim, 2002; p 172.

(37) Prevot, V.; Forano, C.; Besse, J. P.; Abraham, F. *Inorg. Chem.* **1998**, *37*, 4293.

(38) Sideris, P. J.; Nielsen, U. G.; Gan, Z.; Grey, C. P. *Science* **2008**, *321*, 113.

(39) Mohd, Z. H.; Zulkarnain, Z.; Asmah, H. Y.; Dickens, W. V. F. *J. Controlled Release* **2002**, *82*, 417.

(40) Kasha, M.; Rawls, H. R.; El-Bayoumi, M. A. *Pure Appl. Chem.* **1965**, *11*, 371.

JP806024N